

# A Bio-inspired Swimming Robot for Marine Aquaculture Applications: from Concept-design to Simulation

Guoyuan Li<sup>†</sup>, Yuxiang Deng<sup>†</sup>, Ottar L. Osen<sup>‡</sup>, Shusheng Bi<sup>§</sup> and Houxiang Zhang<sup>†\*</sup>

<sup>†</sup>Faculty of Maritime Technology and Operations, Norwegian University of Science and Technology, Aalesund, Norway

{guoyuan.li, yude, hozh}@ntnu.no <sup>‡</sup>Faculty of Engineering and Natural Sciences, Norwegian University of Science and Technology, Aalesund, Norway

ottar.l.osen@ntnu.no <sup>§</sup>Robotics Institute, Beihang University, Beijing, China  
ssbi@buaa.edu.cn

## Abstract

This paper presents the development of a bio-inspired swimming robot from concept design to simulation for marine aquaculture applications. Based on investigation of several fish motions, the Manta ray is found to be the most suitable mock object since the flapping pectoral fin features long-endurance, low noise, high payload capacity, good stability and maneuverability. Through a comprehensive analysis of the structure of Manta ray, the shape proportional relationship between the body and the pectoral fins is obtained. Even though the concept design simplifies the structure, major functional components are retained. By applying two degrees of freedoms to each segment of the pectoral fin, the propulsion mechanism allow the robotic fish to swim in 3D. In addition, a thrust analysis is performed for a good understanding of the fish's aquatic locomotion principle. The flapping motion is decomposed into two orthogonal waves and realized on the robotic fish, taking advantages of sine generators. Simulation experiments including motion comparison, speed and turning tests verify the correctness of the robotic fish's structure and its propulsion mechanisms.

## Index Terms

\* Corresponding author

## I. INTRODUCTION

Marine aquaculture is deeply rooted in Norwegian national economics and traditions. Since the advent of commercial salmon farming around 1970, the aquaculture industry has grown to become the second largest industry in Norway. In order to provide first-hand information about Norwegian aquaculture, sustainable production, food safety, farmed species and the legal framework for aquaculture production, the traditional fishing industry has undergone a number of changes, especially in developing and employing underwater vehicles. Superior capabilities found in natural fish, such as high efficiency, high velocity, silent swimming, high maneuverability and high stability, are the design goals for underwater vehicles used in aquaculture-related applications [1].

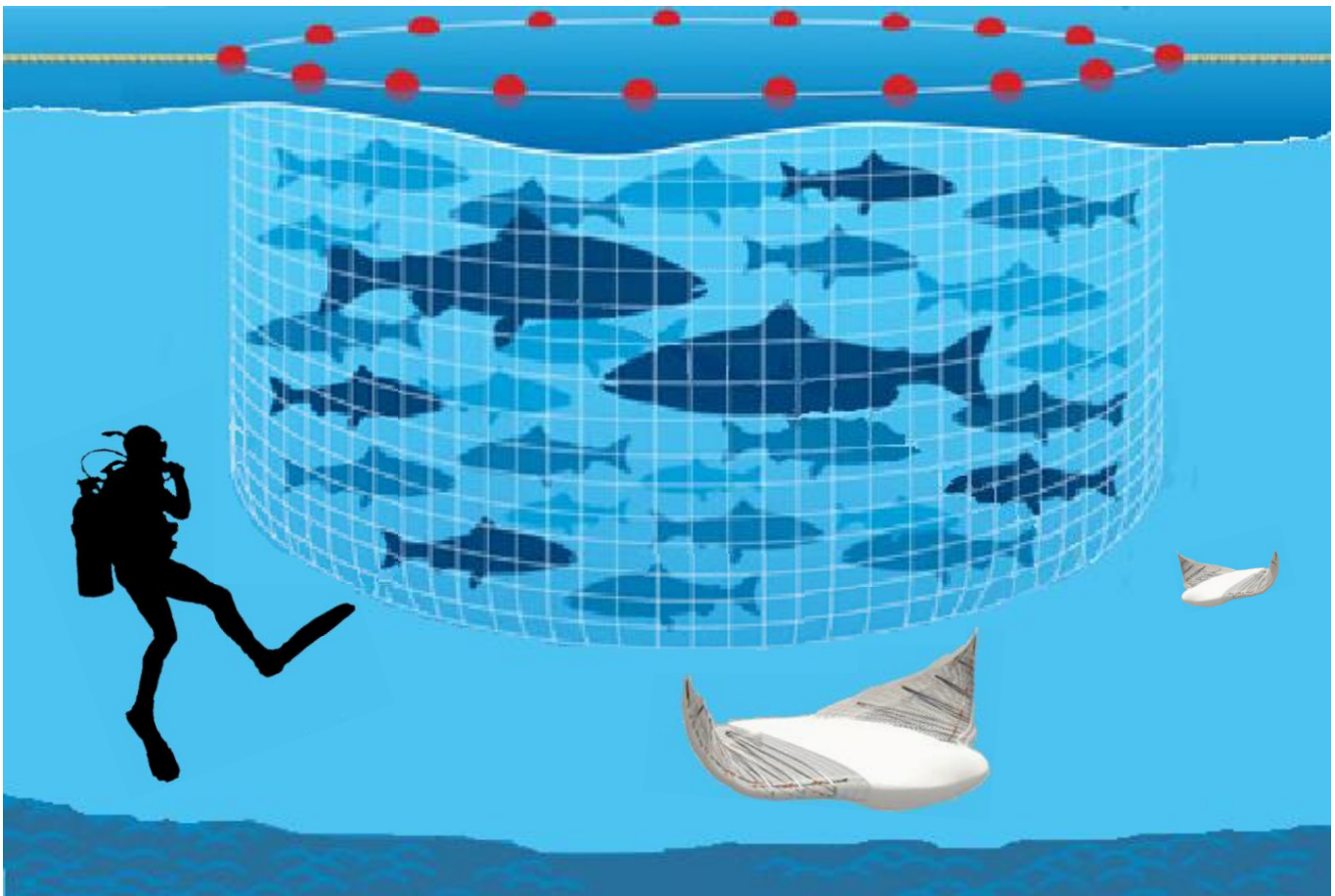


Fig. 1. Concept-design of robotic fish in aquaculture applications.

Nowadays, underwater vehicles are being developed and applied to more and more work in challenging marine environments [2] [3]. Most of the existing underwater vehicles are propeller driven. Even though they are easy to control, their propulsion mode has some drawbacks, such as loud noise, big size, low efficiency, as well as manoeuvring only at low speed. In addition, another significant drawback related to marine aquaculture applications is the acoustic noise caused by the propeller, it inevitably interrupts the cluster of fish and results in low yield. A better alternative is to employ biomimetic technologies in order to develop fish-like robots [4]. Recently, a motion mode from Manta ray has caught the attention of researchers worldwide due to its motion efficiency, manoeuvrability, and stability. Related research based on this motion pattern has been studied and new prototypes of fish-like robots have been developed [5]–[8]. However, current research on this type of fish-like robots focus on propulsive efficiency. How to extract the body features of Manta ray from scratch for modeling and simulation are seldom discussed, but is indeed of great importance to prototype implementation.

Our on-going project aims to develop a biologically inspired robotic fish with practical environmental adaptability and excellent performance in aquaculture inspection applications. At present, fish cage-farming need divers to do calendar inspection of feeding, growth, disease, detection and removal of dead fish, and to verify the cage integrity. A possible substitute for a human diver is a type of fish-like robot inspired from Manta ray, as shown in Fig. 1. The monitoring task can be realized by utilizing sensors such as underwater camera, echo-sounder and side scan sonar on the Manta ray robotic fish. This paper mainly presents the design, modeling and simulation of the robot, with an emphasis on how to efficiently extract features from Manta ray in addition to improve propulsive efficiency.

This paper is organized as follows: Section II briefly compares the motion modes between fish and introduces some famous prototypes of fish-like robots with pectoral fins. Section III introduces the geometrical analysis of the Manta ray based on body shape feature extraction. Section IV present the design and parameterized modeling of the robotic fish. In Section V, simulation with case study is performed for validation of the design. Conclusion and future work are shown in section VI.

## II. RELATED WORK

### A. Comparison of Fish Motion

The fish motion can be classified into two categories according to the major actuation portion of the body: the Body/caudal fins (BCF) mode and Median/paired fins (MPF) mode [9] [10]. More than 85% fish in the world swim by undulating BCF to generate propulsion thrust. More specifically, based on the

TABLE I  
COMPARISON OF THREE SWIMMING LOCOMOTION MODES

Features	Low noise	Speed	Motion efficiency	Stability	Payload capability	Score
Weights	0.25	0.10	0.15	0.25	0.25	
Thunniform	5	5	5	3	3	4.00
Ostraciiform	5	4	4	4	2	3.75
Rajiform	5	3	4	5	5	4.65

difference of undulation in the fraction of their bodies, BCF are further divided into five groups, i.e., Anguilliform, Subcarangiform, Carangiform, Thunniform and Ostraciiform. For the first three motion modes, most of the body participates the swimming oscillation to provide the motion modes with an inferior stability compared to the last two motion modes.

Fish with MPF can also perform undulation or oscillation for propulsion [11]. The Rajiform mode is one of the most stable modes within undulatory MPF and can propel the a with large size and big weight. Manta ray is a typical example of a fish utilizing this aquatic locomotion mode. The oscillatory MPF mode are more like rowing a boat. However, it is not able to support a large and heavy load with long endurance.

Table I lists a comparison of three types of swimming modes which have the potential to be adopted in the new robotic fish design. With respect to the requirements in marine aquaculture applications, we give different weights to each feature. Consequently we give a score to each mode from 5 to 1. The result show that the Rajiform mode best satisfies the needs of marine aquaculture applications.

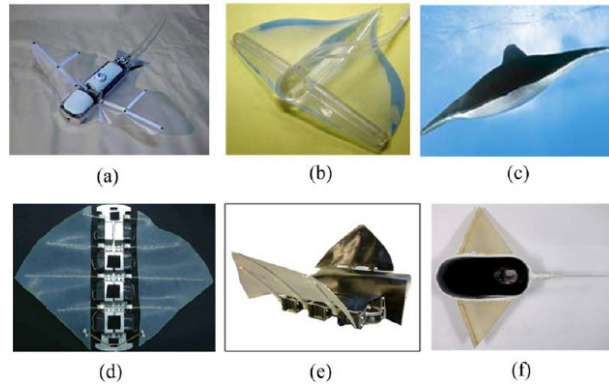


Fig. 2. Developed robotic fish with pectoral fins. (a) Manta ray robot [12]; (b) Rubber manta ray [13]; (c) Aqua-ray [14]; (d) Cow-nosed ray-I [15]; (e) RoMan-II [16]; (f) Micro robot manta ray [17].

### B. Robotic Fish with Pectoral Fins

Robotic fish with pectoral fins has been developed for decades. In 2004, a fish robot mimicking manta ray, developed by a Japanese research team, was demonstrated to the public (Fig. 2a). The body length is 0.65m and the wing span is 0.5m. Suzumori et al. developed a MPF type bionic fish covered by whole soft body and driven by pneumatic cavities (Fig. 2b). It succeeded in mimicking the Manta ray's fins deformations with soft rubber. The Festo company revealed a similar bionic fish called Aqua-Ray that is designed as a mechanical fish covered by seamless deformable skin (Fig. 2c). The total length of the body is 0.615m and the span width is 0.96m. Yang et al. developed "Cow-nosed ray-I" that is composed of a rigid body and two flexible triangular lateral fins with the length of 0.3m and wing span of 0.5m (Fig. 2d). Zhou and Low presented an autonomous underwater vehicle that had inspirations from manta rays, the deformation of the pectoral fin on each side is controlled by several transverse fin rays (Fig. 2e). Wang et al. proposed a micro biomimetic Manta ray robot fish actuated by shape memory alloy wire (Fig. 2f).

Robotic fish prototypes in Fig. 2d and 2e can produce the longitudinal wave along the direction of swimming by means of several transverse fin rays. The complex deformation of pectoral fins is simplified as waves in one direction, which decreases the control difficulty of the pectoral fins to some extent. Despite the simplification the robotic fish retains features like high payload capability, good maneuverability and stability that the real fish have. The other robotic fish prototypes in Fig. 2a,b,c and f share a common feature, the pectoral fin is a single rigid or deformable ray fin. The pectoral fins are made from flexible

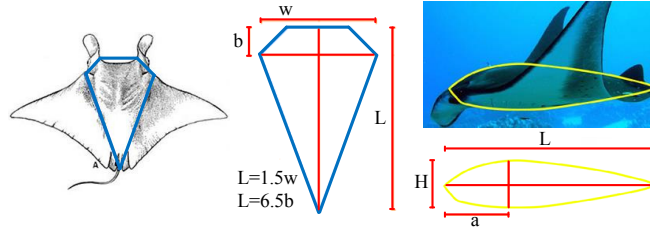


Fig. 3. Geometric abstraction of the body shape.

materials like rubber and silicone. The amplitude and frequency of the single fin ray on each side are the only variables that can be modified.

From aforementioned examples, current research on the Manta-ray-like robots lacks a valid design methodology to bridge the gap from biological mock object to mechanical prototype. In the light of the design methodology from Li et al. [18], the concept design in our project will not only meet the marine aquaculture requirements but also consider the trade-off between modeling and control.

### III. SHAPE ANALYSIS OF MANTA RAY

Manta ray, which is one of the typical aquatic species with Rajiform locomotion mode, has been selected as the biological mocking object of the new designed robotic fish. In nature the structure of Manta rays has evolved into an ideal symmetric form optimising its survival and reproduction. Here, we present a thorough study on its shape for a better understanding of the aquatic locomotion principle.

#### A. Body Structure Analysis

The body shape of manta rays mainly affects its swimming performance in two aspects: 1) the reduction of water resistance, and 2) the stability when swimming. The water resistance is minimized by the streamlined shape which could be observed from lateral view. The flattened diamond shaped body contributes to keep the stability while swimming.

The dorsal and ventral views of the body are diamond shaped. The geometric abstraction of the body from both views is shown in Fig. 3. The longitudinal length  $L$  is adopted as a benchmark in defining

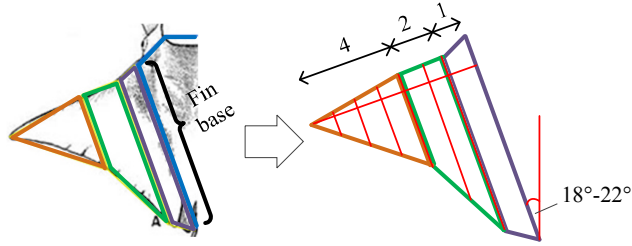


Fig. 4. Geometric abstraction of the pectoral fins from dorsal view.

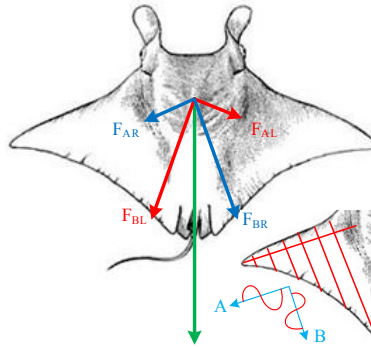


Fig. 5. Demonstration of the forces generated by wave A and B.

the structure. The body shape of the Manta ray can be described as:

$$\begin{cases} w = \frac{2}{3}L \\ b = \frac{2}{13}L \\ H = \frac{2}{9}L \\ a = \frac{1}{3}L \end{cases}$$

where  $w$  is the maximum width of the diamond shape;  $b$  is the distance from the head to the maximum width;  $H$  is the maximum thickness of the body;  $a$  is the distance from the head to the position that reaches the maximum thickness.

The contours from the two views are enough to define the body shape. Thus the contours generalized in this part will be utilized directly in the 3D modeling with CAD programs.

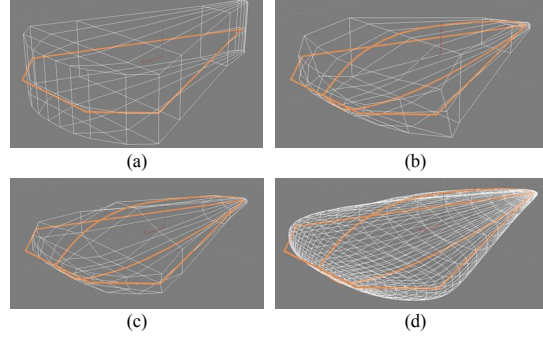


Fig. 6. The body shape design process. (a) Extrude the contour. (b) Reshape the body to be corresponding with the lateral contour. (c) Make a smooth transition. (d) Refine the mesh.

### B. Pectoral Fin Structure Analysis

The pectoral fins are abstracted as a simple triangle at the beginning. However, with the in-depth study, it is found that the shape is over simplified and cannot fully describe the pectoral fins. Therefore, according to the shape of real Manta ray's pectoral fins, the triangle is roughly divided into a combination of three minor components paralleling with the base of the fin, as seen in Fig. 4. A perpendicular from the tip to the base of the fin is drawn for easier observation. The length ratio of the three minor components along the perpendicular is approximate 4:2:1. It indicates that a pectoral fin is possible to refine as seven monospaced segments. The length ratio between the perpendicular and the base is about 1:1.25. The angle between the longitudinal axis of the body and the fin base is within  $18 - 22^\circ$  degrees.

### C. Thrust Analysis

The thrust force of Manta ray is generated by flapping the paired pectoral fins. The deformation caused by the flapping could be decomposed into two waves, as the wave A and B shown in Fig. 5. The wave A is along the direction of pectoral wingspan, as the same as the perpendicular aforementioned previously. Because the calcification of the cartilage decreases from the base of the fin to the tip, the amplitude of the wave A increases accordingly. The wave B is perpendicular to the wave A, along the direction of the fin's base connecting the pectoral fin with the body. Both waves share the same frequency.

$F_{AL}$  and  $F_{BL}$  are forces generated by wave A and B on the left pectoral fin, while  $F_{AR}$  and  $F_{BR}$  are the same for the right pectoral fin. The magnitudes of the forces generated by two waves on each pectoral fin could be changed independently by adjusting the amplitudes of the two waves to form a resultant force along the swimming direction. If the forces on the two fins are different the fish-robot will turn.



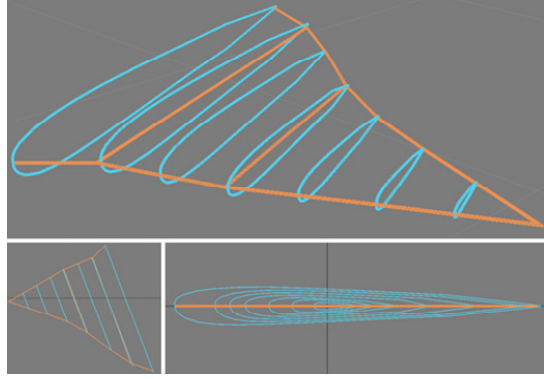


Fig. 7. Frames of the pectoral fin with identical intervals.

Due to the skeletal structure and muscle tissue, the manta rays in nature cannot swim backwards. For the robotic fish it becomes possible to swim backwards since the resultant force comes from the two waves that can generate both forward and backward thrust by adjusting the phases.

#### IV. DESIGN AND MODELING OF MANTA-RAY-LIKE ROBOTIC FISH

From a design point of view, the robotic fish, as a tool for aquaculture inspection, is not required to be as flexible as a real fish. Therefore, a simplified structure with major functional components is the key issue in designing the Manta-ray-like robotic fish. The contours of the body and fins are adopted from the analysis result in Section III. Thus, the proportion of each part comply with the biological structure of Manta ray. The following shows the design and modeling of the robotic fish in 3ds Max [19].

##### A. Body Shaping

First, we import the contours into 3ds Max and set the dimensions. The longitudinal length  $L$ , the maximum body width  $w$  and the maximum body thickness  $H$  are set to  $450mm$ ,  $300mm$  and  $105mm$ , respectively.

The design procedure is shown in Fig. 6. The body shaping starts from the body contour from top view. The contour is redrawn to get a smoother curve in front and a narrow tail at the end. Then it is extruded to the maximum thickness of the body. After that, we reshape the body to be corresponding with the contour from the lateral view. In order to facilitate the further modification, it is better to keep the mesh of the body as simple as possible at this stage. Lastly, we make a smooth transition from the body to the edges of pectoral fins by reducing the thickness of the body from the middle to the lateral.

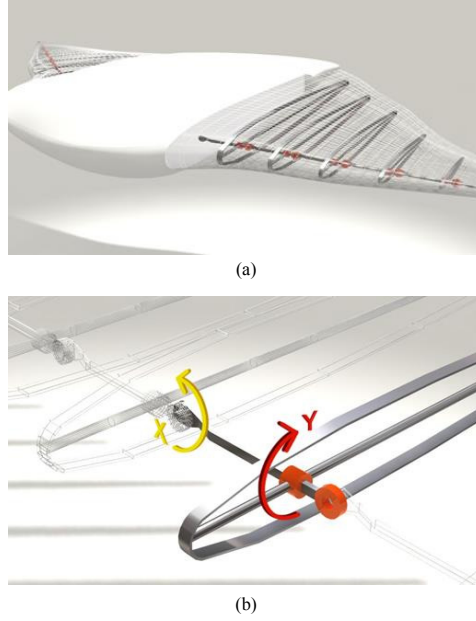


Fig. 8. Propulsion mechanism design. (a) Pectoral fins with divided rigid segments. (b) Single segment with two DOFs in rotation.

### B. Pectoral Fins Shaping

The shapes of the pectoral fins are modeled by creating several frames at identical intervals, as shown in Fig. 7. The lengths of the frames are restrained by the contour of the fins. In order to get a better hydrodynamic performance, the lateral views of the frames are torpedo-shaped. The next step is to create the mesh in accordance with the frames. Thus the frames will be utilized to fully control the deformation of the fins. As with the body shaping, the last step is to refine the mesh to get a smooth surface.

### C. Propulsion Mechanism Design

As mentioned in Section III-C, there are two waves on the pectoral fins along two directions. These two waves should be brought out by the rigid mechanism so that the deformation could be fully controlled. To this end, the pectoral fin is divided into seven segments and each of the segment is supported by a torpedo-shaped frame, as shown in Fig. 8a. The propulsion mechanism on the frame has two degrees of freedoms (DOFs), as illustrated in Fig. 8b. Thus the assembly of the seven segments can generate the motion in 3D.

To realize the swimming motion of Manta rays, the control sequence of these segments needs to be considered. Theoretically, the mechanism is able to generate the deformation in two directions by

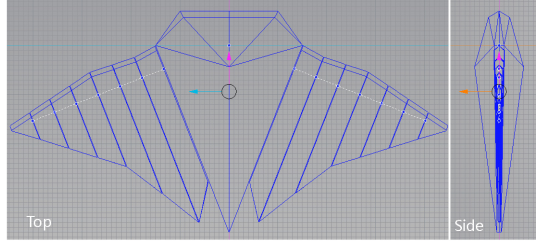


Fig. 9. Simplified 3D model for robotic fish simulation.

rotating the joints back and forth with a fixed phase difference. In biology, a group of neural circuits called central pattern generators (CPG) in the spinal cord of vertebrates is proved to be responsible for producing coordinated patterns of rhythmic activity [20]. In robotics, CPG has been applied on bio-inspired robots for gait generation [21]–[23]. Here, we follow [23] and use the sine generator as the propulsion mechanism:

$$\begin{cases} \theta_A(i, t) = O_A(i, t) * \sin(\omega t + \psi_A(i)) & i \in \{1, 2, \dots, 7\} \\ \theta_B(i, t) = O_B(i, t) * \sin(\omega t + \psi_B(i)) & i \in \{1, 2, \dots, 7\} \end{cases}$$

where  $\theta$  is the reference angle for the joint;  $O$ ,  $\omega$  and  $\psi$  represent the amplitude, the angular frequency and the phase, respectively. Thus, the propulsion mechanism is completed.

## V. SIMULATION

### A. Design Verification

To verify the feasibility of the designed robotic fish, a simulation was carried out in AgX dynamics [24]. AgX is powerful for physical simulation, including hydrodynamics. In this simulation, the gravity is set to  $-9.81m/s^2$  to be consistent with the real world. To keep the robotic fish remaining under the water its density is set to be the same as the density of water and its center of mass is placed a little bit lower than the geometric center. Pressure drag, lift and viscous drag coefficients are set as 1.0, 0.02 and 0.0 respectively. The simplified 3D model for simulation is built in Blender [25] and then imported into AgX, as shown in Fig. 9. The shapes of the body and fins are abstracted from real manta ray as discussed before.

In the simulation, the two body waves for producing angle reference are set as  $O_A = 0.10$ ,  $O_B = 0.25$ ,  $\omega = 0.25$ ,  $\psi_A = 0.33$  and  $\psi_B = 0$ . A PD controller is used to follow the reference. A comparison of

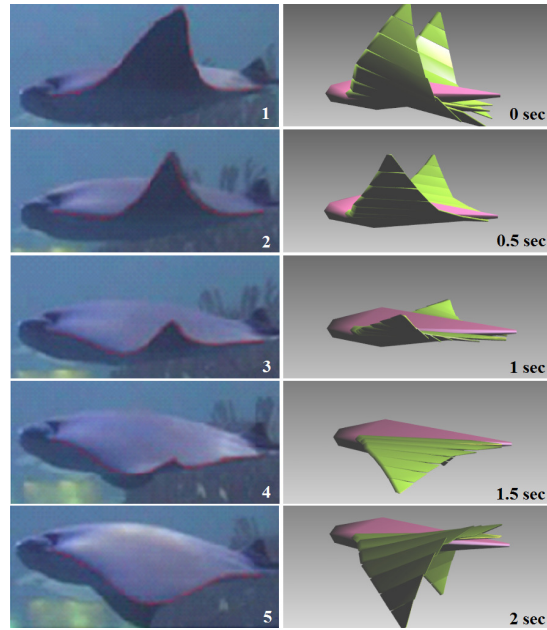


Fig. 10. Snapshots of the real Manta ray and the simulated robotic fish.

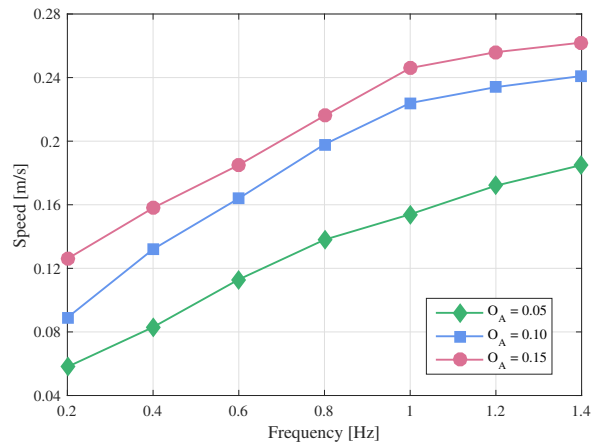


Fig. 11. Forward swimming speed test.

pectoral fins deformation between the real Manta ray and the simulated robotic fish was carried out to validate the concept robotic fish design. Fig. 10 are snapshots of the real and the simulated Manta ray in half a period. Note that the time intervals for the snapshots are the same. The result shows that not only the structure but also the swimming pattern of the real Manta ray are successfully duplicated to the robotic fish.

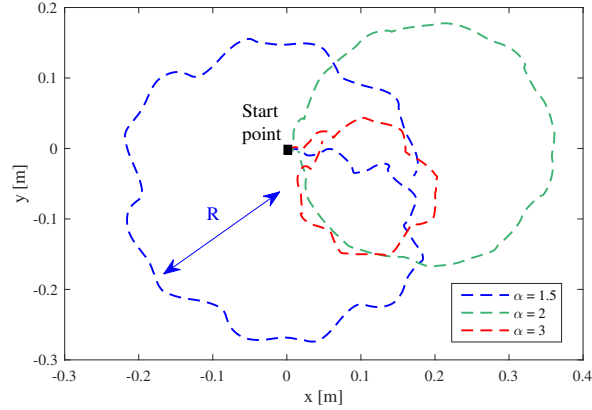


Fig. 12. Forward turning test.

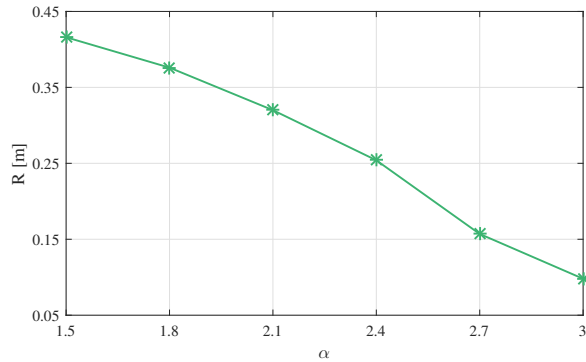


Fig. 13. Variation of turning radius with respect to amplitude ratio.

### B. Maneuverability Test

We also performed simulations to verify the maneuverability of the robotic fish. The forward swimming speed was tested by utilizing the same values of the two body waves used in the previous experiment, but with different amplitudes and frequencies, as shown in Fig. 11. The speed increases monotonically with increasing amplitude and frequency. The tracking error of the PD controller also increases due to motor torque limit. The speed increment therefore decreases as the frequency increases. The highest speed at 1.4Hz is approximately 0.262m/s, which corresponds to 0.58 bodylength/s.

To evaluate the turning ability, we define the ratio of amplitude between the left and right pectoral fins as  $\alpha$ .  $\alpha$  is a value no less than 1, which indicates the degree of curvature. During the turning, the inner turning fin's amplitude is fixed as  $O_A = 0.05$ , while the other fin's amplitude is therefore  $O_A = 0.05\alpha$ . Fig. 12 shows the trajectory of different turning strategies. The turning ability is determined by the

turning radius  $R$ : the smaller the radius  $R$ , the sharper turning it achieves. We only tested the change of  $\alpha$  from 1.5 to 3, since further increasing  $\alpha$  will decrease the swimming stability. Fig. 13 illustrates that the turning radius  $R$  decreases monotonically with the amplitude ratio  $\alpha$ . The sharpest turning is obtained at  $\alpha = 3$ , where the radius of the curvature is about 0.098m. Compared to the width of the robot, the robot features a good steering ability.

## VI. CONCLUSION

In this paper we have presented how to develop a bio-inspired swimming robot from concept design to simulation. First, according to the demands in marine aquaculture applications, superior capabilities performed by Manta rays are investigated. Then, the body, the pectoral fin and the propulsion mechanism of Manta rays are thoroughly analyzed. Next, a simplified design of Manta-ray-like robotic fish is studied. The body is a diamond shape and the pectoral fin is consists of seven segments. The propulsion of the robot is achieved by applying the sine generator to each of the segment. Lastly the simulation results show that the proposed approach for robotic fish design is correct and effective in realizing flapping swimming.

Future work will focus on two aspects: (1) Refining the pectoral fins, aiming to maximize the propulsion while reducing power consumption. (2) Optimizing the CPG generation algorithm to increase the maneuverability.

## ACKNOWLEDGEMENT

The research of the bio-inspired swimming robot is a joint project collaborated with Beihang University, and partially supported by the Mechatronics Lab at the Faculty of Maritime Technology and Operations, NTNU i Aalesund.

## REFERENCES

- [1] P. G. Lee, "A review of automated control systems for aquaculture and design criteria for their implementation", *Aquacultural Engineering*, vol. 14, no. 3, pp. 205-227, 1995.
- [2] K. H. Low, C. W. Chong and C. Zhou, C, "Performance study of a fish robot propelled by a flexible caudal fin", in *Proc. of IEEE Int. Conf. on Robotics and Automation (ICRA)*, Alaska, pp. 90-95, 2010.
- [3] W. S. Chu, K. T. Lee, S. H. Song, M. W. Han, J. Y. Lee, H. S. Kim, M. S. Kim, Y. J. Park, K. J. Cho and S. H. Ahn, "Review of biomimetic underwater robots using smart actuators", *International Journal of Precision Engineering and Manufacturing*, vol. 13, no. 7, pp. 1281-1292, 2012.
- [4] R. Du,, Z. Li, K. Youcef-Toumi and P. V. Y Alvarado, *Robot fish: bio-inspired fishlike underwater robots*, Springer, 2015.

- [5] A. Punning, M. Anton, M. Kruusmaa and A. Aabloo, A, “A biologically inspired ray-like underwater robot with electroactive polymer pectoral fins”, in *Proc. of Int. IEEE Conf. on Mechatronics and Robotics*, Aachen, Germany, pp. 241-245, 2004.
- [6] Y. Cai, S. Bi and L. Zheng, “Design and experiments of a robotic fish imitating cow-nosed ray”, *Journal of Bionic Engineering*, vol. 7, no. 2, pp. 120-126, 2010.
- [7] S. Bi, C. Niu, Y. Cai, L. Zhang and H. Zhang, “A waypoint-tracking controller for a bionic autonomous underwater vehicle with two pectoral fins”, *Advanced Robotics*, vol. 28, no. 10, pp. 673-681, 2014.
- [8] C. Zhou and K. H. Low, “Design and locomotion control of a biomimetic underwater vehicle with fin propulsion”, *IEEE/ASME Transactions on Mechatronics*, vol. 17, no. 1, pp. 25-35, 2012.
- [9] R. W. Blake, “Fish functional design and swimming performance”, *Journal of fish biology*, vol. 65, no. 5, pp. 1193-1222, 2004.
- [10] G. V. Lauder, “Fish locomotion: recent advances and new directions”, *Annual review of marine science*, vol. 7, pp. 521-545, 2015.
- [11] L. J. Rosenberger, “Pectoral fin locomotion in batoid fishes: undulation versus oscillation”, *Journal of Experimental Biology*, vol. 204, no. 2, pp. 379-394, 2001.
- [12] Manta ray robot [Online]. Available: <http://www.imae-kagaku.com/mech.htm>. [Accessed: Feb. 20, 2016].
- [13] K. Suzumori, S. Endo, T. Kanda, N. Kato and H. Suzuki, “A bending pneumatic rubber actuator realizing soft-bodied manta swimming robot”, in *Proc. of IEEE Int. Conf. on Robotics and Automation (ICRA)*, Roma, Italy, pp. 4975-4980, 2007,
- [14] Festo, “Manta ray robot can loop-the-loop”, *New Scientist*, vol. 195, no. 2622, pp. 27, 2007.
- [15] S. B. Yang, J. Qiu and X. Y. Han, “Kinematics modeling and experiments of pectoral oscillation propulsion robotic fish”, *Journal of Bionic engineering*, vol. 6, no. 2, pp. 174-179, 2009.
- [16] C. Zhou and K. H. Low, “Better endurance and load capacity: an improved design of manta ray robot (RoMan-II)”. *Journal of Bionic Engineering*, vol. 7, pp. 137-144, 2010..
- [17] Z. Wang, Y. Wang, J. Li and G. Hang, “A micro biomimetic manta ray robot fish actuated by SMA”, in *Proc. of IEEE Int. Conf. on Robotics and Biomimetics (ROBIO)*, Guilin, China, pp. 1809-1813, 2009.
- [18] G. Li, W. Li, J. Zhang and H. Zhang, “Analysis and design of asymmetric oscillation for caterpillar-like locomotion”, *Journal of Bionic Engineering*, vol. 12, no. 2, pp. 190-203, 2015.
- [19] 3Ds Max [Online]. Available: <http://www.autodesk.com/products/3ds-max/overview>. [Accessed: Feb. 20, 2016].
- [20] S. Grillner, “Neurobiological bases of rhythmic motor acts in vertebrates”, *Science*, vol. 228, pp. 143-149, 1985.
- [21] A. J. Ijspeert and A. Crespi, “Online trajectory generation in an amphibious snake robot using a lamprey-like central pattern generator model”, in *Proc. of IEEE Int. Conf. on Robotics and Automation (ICRA)*, Roma, Italy, pp. 262-268, 2007.
- [22] G. Li., H. Zhang, J. Zhang and H. P. Hildre, “An Approach for Adaptive Limbless Locomotion Using a CPG-Based Reflex Mechanism”, *Journal of Bionic Engineering*, vol. 11, no. 3, pp. 389-399, 2014.
- [23] J. G. Gómez, *Modular robotics and locomotion: application to limbless robots*, Ph.D. dissertation, Universidad Autonoma de Madrid, Madrid, 2008.
- [24] A. Backman, “Algoryx—Interactive Physics”, in *Proc. of the annual SIGRAD conference special theme: interaction*, Stockholm, Sweden, pp. 87-87, 2008.
- [25] Blender [Online]. Available: <https://www.blender.org/>. [Accessed: Feb. 20, 2016].